PHYSE 5182
pp: 1--7 (col.fig.: Nil)
PROD. TYPE: COM
ED: JSS
PAGN: Murthy.N – SCAN: Profi

ELSEVIER

Physica E 000 (2001) 000–000

PHYSICA E

www.elsevier.com/locate/physe

Electron spectrum and infrared transitions in semiconductor superlattices with a unit cell allowing for quasi-localised carrier states

A.V. Dmitriev[a, *], R. Keiper[b], V.V. Makeev[a]

[a] *Department of Low Temperature Physics, Faculty of Physics, Moscow State University, Moscow, 119899, Russia*
[b] *Institut für Physik, Humboldt–Universität zu Berlin, Invalidenstr. 110, 10115 Berlin, Germany*

Abstract

We studied theoretically, the electron spectrum and infrared transitions in a superlattice with a unit cell allowing for quasi-localised carrier states. The dispersion relation and the band structure of such a system have been found. We calculated the dipole matrix element for inter-subband carrier infrared transitions. The wave functions and the electron spectrum in this superlattice show a peculiarity when the energy of a band state approaches the energy of the quasi-localised state in the single cell. The absorption strength peaks up at the respective frequencies. © 2001 Published by Elsevier Science B.V.

PACS: 78.66.−w; 73.20.Dx; 71.15.Ap

Keywords: Superlattice; Resonant states; IR-transitions

1. Introduction

Usually, one assumes that in semiconductors, along with other crystals, an electron state belongs to one of the two possible kinds. Namely, it can be either a Bloch band state, or a localised state residing in the forbidden gap. However, a third kind of carrier states, resonant or quasi-localised [1], has been shown to play a significant role in a number of occasions. These states, long before known both in optics [2] and in quantum mechanics [3], appear in semiconductors e.g., when an impurity level, split off from one band, overlaps with another allowed band, or when a deep impurity level overlaps with one of the allowed energy bands. In certain conditions, resonant states may significantly affect the kinetic properties of a semiconductor [4,5].

Quasi-localised states may be present in artificially prepared heterostructures, e.g. in two-barrier quantum well systems. We have shown earlier [6] that in their presence the absorption coefficient significantly increases in the frequency range of the intraband transitions into the resonant state. Since the latter state

* Corresponding author. Fax: +7-095-932-88-76.
E-mail address: dmitriev@1t.phys.msu.su (A.V. Dmitriev).

1386-9477/01/$ - see front matter © 2001 Published by Elsevier Science B.V.
PII: S1386-9477(01)00220-X

formally belongs to the continuum, one can expect it to decay easily into a delocalised wave, so that no strong electric field would be required to add the excited electron to an observable photocurrent. Hence, heterostructures with quasi-localised states sound quite appealing as candidates for selective quantum well infrared photodetectors (QWIPs). These detectors would combine high spectral selectivity with low dark current because of low bias applied. Such combination is hardly attainable with conventional QWIPs, where the working transition goes to a bound state, or in the opposite case, to a plain continuum state (see the review article [7]).

In the cited paper [6], we discussed infrared optical properties of a single quantum well system. However, arrays of quantum wells or superlattices are normally used for experimental purposes and practical applications. Thus, we thought it relevant to consider a periodic structure composed of quantum wells with resonant states. How the adjacent resonant states interfere with each other and with the continuum states may be a matter of independent theoretical interest. To the best of our knowledge, neither infrared optical properties nor subband spectrum of this kind of superlattices have been considered before. This is the goal of the present paper.

The theoretical approach to the electronic spectrum of superlattices is well developed (see e.g. Refs. [8,9]). In Ref. [10] a detailed spectral analysis of a conventional AB superlattice (two alternating layers) has been demonstrated. We use a similar approach to analyse the electronic spectrum of a superlattice with a more complex unit cell.

2. Model

We consider one non-degenerate band, let it be the conduction band, of a semiconductor superlattice, where each cell is described within the effective-mass approximation by a one-dimensional model potential as follows (see also Fig. 1):

$$U(x) = \left\{ \begin{matrix} -V, & 0 < x < a \\ 0, & a < x < b \end{matrix} \right\} + \Omega\,[\delta(x) + \delta(x-a)], \tag{1}$$

where x is the growth direction of the superlattice, a and b are the well width and the structure period,

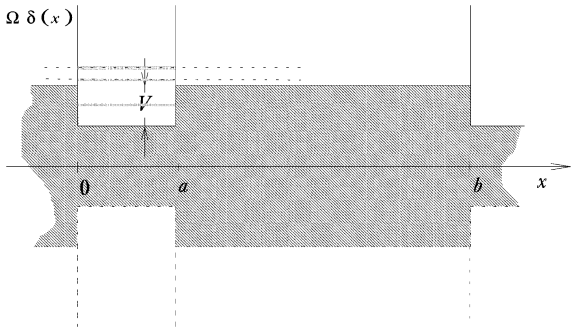

Fig. 1. The considered model potential. Please note the additional δ-barriers surrounding the well. Several lower subbands are marked. One subband is supposed to remain below the top of the main barriers, the rest being above.

respectively, V is the well depth. δ-like barriers on the well's edges represent a simplified approximation of additional real barriers of finite width and height that would surround each well. The parameter Ω thus represents the reverse tunnel transparency of the real barrier. The main barriers of width $(b-a)$ separate the wells. The potential in Eq. (1) is assumed to be 0 at the top of the main barrier.

It is clear that the infinitely high and infinitely thin δ-barriers, surrounding the wells, cannot be grown up in a real heterostucture. In real structures, all barriers have finite height and width. However, the δ-function approximation of real barriers adopted in Eq. (1) is a well-known simplified method used in a number of quantum-mechanical problems (see, for example [11]). It corresponds to a very high and thin barrier with finite penetrability. From the point of view of the problem, we consider here, the main difference between the δ-barrier and the real one is an infinite height of the former. As a result, our model system has an infinite set of quasi-localised states (resonances) whereas a real structure hardly can produce more than one or two of them. But as far as we are interested in the properties of a single resonance, the δ-approximation leads to qualitatively correct and physically meaningful results.

If all the structure consisted of only one quantum well with potential (1), we might speak of quasi-localised electronic states in its spectrum. These states appear on an energy scale close to truly localised states that would exist in the well,

if the additional barriers (walls) were absolutely impenetrable. Finite penetrability of the walls transforms the truly localised size-quantised states into quasi-localised states. Of course, this matters only for the excited states lying above the top of the main barriers, like the two higher levels in Fig. 1. The lower ground state in the single quantum well is always localised.

Turning back to the periodic heterostructure, let us see how the resonant states affect the properties of the whole system. The envelope wave functions may be represented as

$$\Psi(x)=\begin{cases} A_1 e^{iqx}+A_2 e^{-iqx}, & 0<x<a,\\ B_1 e^{i\kappa x}+B_2 e^{-i\kappa x}, & a<x<b,\end{cases}$$

$$\Psi(x+b)=e^{ikb}\Psi(x), \tag{2}$$

where $q=(1/\hbar)\sqrt{2m(E+V)}$, $\kappa=(1/\hbar)\sqrt{2mE}$, E is the particle energy counted from the top of the main barrier, m is the effective mass, kb is the phase shift of the envelope function, resulting from a one-lattice-period displacement along the growth direction. Ignoring the changes in the effective mass across the superlattice layers, we obtain a conventional boundary condition on the left-hand border of the well ($x=0$):

$$\begin{cases} \Psi(x)|_{0-}^{0+}=0,\\ \dfrac{d}{dx}\ln\Psi(x)|_{0-}^{0+}=\Omega.\end{cases}$$

Having written similar boundary conditions for the right-hand border ($x=a$), we come to a homogeneous system of equations defining the coefficients in Eq. (2):

$$\begin{pmatrix} e^{ikb} & e^{ikb} & -e^{i\kappa b} & -e^{-i\kappa b}\\ (q+i\Omega)e^{ikb} & (-q+i\Omega)e^{ikb} & -\kappa e^{i\kappa b} & \kappa e^{-i\kappa b}\\ e^{iqa} & e^{-iqa} & -e^{i\kappa a} & -e^{-i\kappa a}\\ (-q+i\Omega)e^{iqa} & (q+i\Omega)e^{-iqa} & \kappa e^{i\kappa a} & -\kappa e^{-i\kappa a}\end{pmatrix} \times \begin{pmatrix} A_1\\ A_2\\ B_1\\ B_2\end{pmatrix}=0.$$

A non-zero solution of this system exists only if the system determinant is zero, hence we obtain the dispersion relation

$$\cos kb=\frac{\Omega^2-q^2-\kappa^2}{2\kappa q}\sin\kappa(b-a)\sin qa+\frac{\Omega}{q}\cos\kappa(b-a)\sin qa+\frac{\Omega}{\kappa}\sin\kappa(b-a)\cos qa+\cos\kappa(b-a)\cos qa. \tag{3}$$

The energy intervals, where the absolute value of the right-hand side of Eq. (3) does not exceed unity, correspond to allowed subbands of our superlattice. Unfortunately, no analytic solution for the wave function coefficients in Eq. (2) can be obtained at arbitrary k, so further spectrum calculations were performed numerically.

3. Spectrum, wave functions and momentum matrix element

Fig. 2 depicts the envelope wave functions of several adjacent subbands. The lower plot represents a wave function belonging to the lowest subband; this band originates from the well's ground state. Naturally, electronic density concentrates within the well's limits. The shape of the wave functions within the well practically does not depend on k; only the phase shift between adjacent cells changes with k.

The rest of the wave functions in Fig. 2 corresponds to positive energy values. Most of these have electronic density concentrated just outside the wells. We can roughly infer that these functions originate from electronic states residing over the barriers. The additional δ-barriers, surrounding the wells, prevent the particles from entering the latter.

Note that the functions on the edges of each subband have definite parity when viewed from both well centre or barrier centre, in agreement with general rules established in Ref. [12] for wave functions in periodic structures with symmetric potential. The wave functions on the edges of the ground subband are both even about the well centre, but when viewed from the barrier centre, the $k=0$ function is even and the $k=\pi/b$ one is odd. This can be easily understood in full

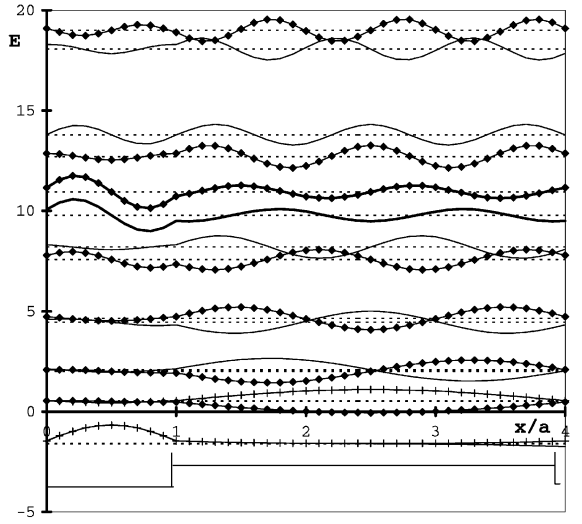

Fig. 2. The subband structure of the superlattice for $b/a = 4$, $V = 1.47$ and $\Omega = 8$. The energy unit is $\hbar^2/ma^2$. The subband edges are marked by horizontal dotted lines. Solid curves represent the envelope functions at the band edges, of which the states with $k = 0$ are marked with rhombuses. Two thick solid curves represent the functions of the 'resonant' subband. In this subband, electron density resides mainly within the wells, and both subband edge states are odd about the well centre. The unit cell potential is shown below.

analogy to the tight-binding model [13] with the lowest electron states in the wells taken as a basis. On the contrary, in most higher subbands both wave functions on the band edges have the same parity about the barrier centre and different parities about the well centre. This is because they are made up mainly of the electron states that reside over the barriers as explained above. For definiteness, further on we speak of parity about the well centre.

However, there is an excited subband, with energy close to the resonant value in the wells, with properties that resemble the ground subband. Let us call this subband resonant. Here electron density is large within the well limits, and the envelope functions have the same parity on the band edges. Their structure resembles the structure of the functions in the lowest subband, which originated from the localised states in the wells. Similarly, the resonant band is built from the quasi-localised electron states between the additional barriers. The quasi-localised states are mainly concentrated within the wells, so the structure of the corresponding resonant subband is much like that of the ground subband.

Henceforth, we can expect the dipole matrix element of the optical transition between these two bands, ground and resonant, to be anomalously large, because of high overlap between the wave functions in the two bands. Then the absorption coefficient would also increase. The energy of corresponding transitions in common superlattices lies in the infrared range.

In our calculations, we used $|p_n(k)|^2$, the momentum matrix element squared, as a convenient straightforward parameter, characterising the absorption per one electron in the ground subband (see Section 4). $|p_n(k)|^2$ is the matrix element between wave functions in the lowest and nth subbands taken at one Bloch vector value k (because of negligible photon's momentum, we can consider the electron transitions vertical). The derivative parameters, such as absorption probability or absorption coefficient α, are proportional to $|p_n(k)|^2$.

Figs. 3 and 4 depict the dependence of $|p_n|^2$ on the energy of the final electron state at two different values of superlattice period. The variation of other superlattice parameters (a, Ω, V) does not change the qualitative picture. We can see first that the transition matrix element goes up in a number of subbands in the area of resonance. Secondly, absorption is maximum at one edge and drops almost to zero at another edge of the subband. This is true for all subbands except the resonant. While before the resonance absorption

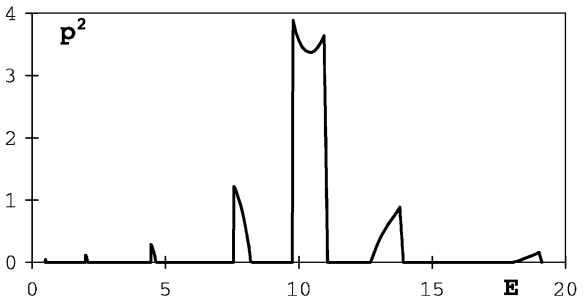

Fig. 3. The momentum matrix element squared for the same system as in Fig. 2. Absorption in subbands preceding the resonant subband drops from the lower edge to the higher. When the resonant band is passed, the picture reverses. The energy unit is $\hbar^2/(ma^2)$, and the matrix element squared is measured in $\hbar^2/a^2$.

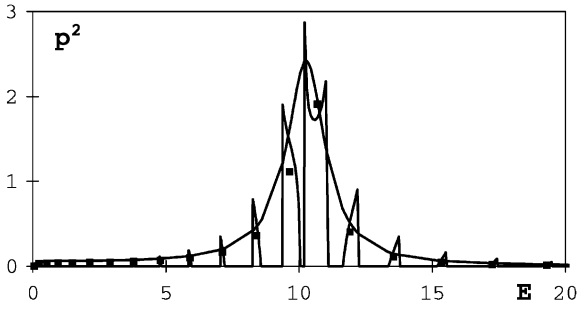

Fig. 4. The same dependence as in Fig. 3, but for thicker main barriers: $b/a = 10$. The well depth $V = 1.47$. Full squares show the ratio of $\langle |p_n|^2 \rangle / (E_n - E_{n-1})$, that is, the averaged over an energy interval matrix element squared, for the superlattice. Smooth curve represents the product of square of the momentum operator matrix element by the density of final states, $|p_{if}|^2 \rho$, in a single quantum well according to [6].

monotonously goes down from the lower edge to the upper, after the resonance the picture become reversed. Matching the picture with Fig. 2, we see that when absorption is maximum, the final wave function has 'proper' parity, i.e. the opposite to the parity of the ground state. In the resonant band parity is 'proper' on both band edges, and band absorption spectrum has different shape.

The picture reflects the hybrid structure of the electronic spectrum of the considered superlattice. In the given configuration, where main barriers are thicker than wells, the excited subband spectrum is formed mainly by barrier levels. An 'intrusion' of the resonant level from the well confuses the monotonous pattern and upturns parity switching order.

As the interwell distance increases, the transition matrix elements drop down but simultaneously the density of subbands per energy interval increases so that if one considers the absorption averaged over an energy interval containing many bands

$$\alpha(\omega)\,\Delta\hbar\omega \sim \sum_{n \in \Delta\hbar\omega} \langle |p_n|^2 \rangle,$$

then this quantity varies only weakly. Here $\langle |p_n|^2 \rangle$ is the transition matrix element averaged over all states in the nth subband, and summation goes over all subbands that enter the $\Delta\hbar\omega$-wide interval of final energies. Remember that the number of single-particle states in a subband is determined only by the number of the superlattice periods, and not by the band width.

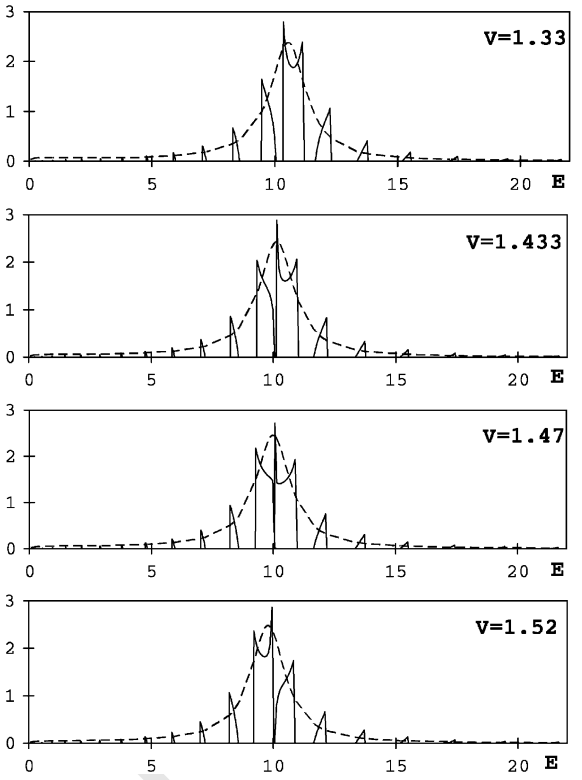

Fig. 5. The change of $|p_n|^2$ for the system of Fig. 4 under variation of V, the well depth: (a) $V = 1.33$, (b) 1.433, (c) 1.47, (d) 1.52.

It is interesting to observe the superlattice energy spectrum and absorption variations over the parameter region where the resonant state leaves one subband and enters another. Fig. 5 illustrates this process at the variation of the well depth. One can see how the absorption peak moves from one subband to another and follow the corresponding changes of the absorption band shapes: the property to be 'resonant' goes from the subband to its neighbour.

4. Absorption strength

Using the momentum matrix element data shown above one can easily calculate such physical quantity of interest as the absorption probability due to an electron transition from the ground subband to a higher subband n. The standard perturbative approach for a transition probability at one photon absorption (see,

for example, [14,15]) gives the absorption probability as

$$W_{\mathrm{fi}} = \frac{2\pi}{\hbar}|\hat{H}^{\mathrm{int}}_{\mathrm{fi}}|^2\delta(\varepsilon_{\mathrm{f}} - \varepsilon_{\mathrm{i}} - \hbar\omega)$$

$$= \frac{2\pi e^2}{m^2c^2\hbar}A_0^2\,|p_{\mathrm{fi}}|^2\delta(\varepsilon_{\mathrm{f}} - \varepsilon_{\mathrm{i}} - \hbar\omega)$$

$$= \left(\frac{2\pi e}{m}\right)^2 \frac{N(\omega)}{\omega c}\,|p_{\mathrm{fi}}|^2\delta(\varepsilon_{\mathrm{f}} - \varepsilon_{\mathrm{i}} - \hbar\omega)$$

$$= \left(\frac{2\pi e}{m}\right)^2 \frac{I(\omega)}{\hbar\omega^2 c}\,|p_{\mathrm{fi}}|^2\delta(\varepsilon_{\mathrm{f}} - \varepsilon_{\mathrm{i}} - \hbar\omega), \qquad (4)$$

where subscripts i, f stand for initial and final state, respectively;

$$\hat{H}^{\mathrm{int}} = -\frac{e}{mc}\mathbf{A}\hat{\mathbf{p}}$$

is the interaction Hamiltonian with electromagnetic field, **A** being the vector potential of the latter with the amplitude $A_0(\omega)$, and $\hat{\mathbf{p}}$ being the electron momentum operator; the photon flux density $N(\omega)$ satisfies the relation $A_0^2(\omega) = (2\pi\hbar c/\omega)N(\omega)$; $I(\omega) = \hbar\omega N(\omega)$ is the radiation spectral intensity. It was assumed in Eq. (4) that the superlattice length is small as compared with the radiation wavelength, which seems reasonable for the infrared intraband transitions we considered here.

On the other hand, as the superlattice we consider is not too long, we will assume that each subband Bloch level can be spectrally resolved separately from the others. Assuming also that the light beam spectral width covers only one possible transition from a Bloch state in the ground subband into another Bloch state in an excited subband, after the integration over the incident radiation frequency one obtains, taking into account also the initial and final electron state degeneracy due to the perpendicular (in-plane) electron motion [1].

$$W(\omega_{\mathrm{fi}}) = 2\sum_{k_y,k_z}\mathscr{P}\left(\frac{2\pi e}{m}\right)^2 \frac{I(\omega_{\mathrm{fi}})}{\hbar^2\omega_{\mathrm{fi}}^2 c}\,|p_{\mathrm{fi}}|^2, \qquad (5)$$

where $\omega_{\mathrm{fi}} = (\varepsilon_{\mathrm{f}} - \varepsilon_{\mathrm{i}})/\hbar$ is the transition frequency, and $\mathscr{P}$ is the statistical factor describing the electron Fermi distribution in the ground subband. The electron momentum conservation at an optical transition has been taken into account in this equation. Factor 2 reflects the spin degeneracy.

[1] The degeneracy is connected with the neglect of the electron effective mass difference in the layers of the superlattice. As a result, in-plane energy dispersion laws are similar in all subbands. This is true for doped superlattices, and for compositional ones this is an approximation.

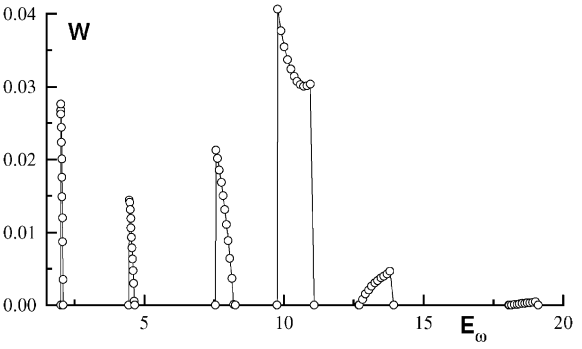

Fig. 6. Light absorption probability vs photon energy for the system of Fig. 3. Each point corresponds to a transition between two Bloch electron states, one in the ground subband, the other in an excited one. The line is a guide for the eye. The energy unit is $\hbar^2/(ma^2)$, the probability is in arbitrary units.

Performing the elementary summation in Eq. (5), one comes finally to the expression for the light absorption probability at the electron transition between two Bloch subband states, one in the ground subband and the other in an excited one.

$$W(\omega_{\mathrm{fi}}) = \frac{2\pi}{c}\left(\frac{e}{\hbar^2\omega_{\mathrm{fi}}m}\right)^2 I(\omega_{\mathrm{fi}})\,p_{\mathrm{F}\perp}^2\,|p_x|^2$$

$$= \left(\frac{2\pi e}{\hbar\omega_{\mathrm{fi}}m}\right)^2 \frac{I(\omega_{\mathrm{fi}})}{c}\,N_{2\mathrm{d}}\,|p_x|^2, \qquad (6)$$

where $p_{\mathrm{F}\perp}$ is the 2D in-plane Fermi momentum of electrons in the ground subband; $N_{2\mathrm{D}}$ is the corresponding sheet electron density in a layer of the superlattice; the light beam is directed along the superlattice layers with its polarisation parallel to the growth axis x to ensure maximum absorption.

Formula (6) gives the connection between the absorption strength and $|p_z|^2$ and clearly shows that the absorption strength reflects all the peculiarities of the matrix element discussed above (see Fig. 6). Other physical quantities such as the cross-section of the photon absorption, absorption coefficient, etc., can be calculated similarly [6].

5. Comparison with properties of a single well

An analytic calculations have been performed in Ref. [6] for a single well heterostructure with the same model potential as in Eq. (1). One could expect that the current results should fit to the conclusions of Ref. [6] in the limit of remote wells, i.e. for a long-period superlattice with $b/a \gg 1$.

We can employ $|p_n|^2\rho$ as a variable characterising optical absorption per one electron in a single quantum well, where $|p_n|^2$ is the momentum matrix element squared, and ρ is the density of final states. An analogous parameter for a superlattice is $\langle|p_n|^2\rangle/(E_n - E_{n-1})$, where $\langle\ldots\rangle$ stands again for the averaging over the states in nth subband, and E_n is the energy of the middle state in the subband (when $kb = \pi/2$). Thus $(E_n - E_{n-1})$ is approximately the distance between adjacent bands. This parameter characterises the absorption in the area of nth subband, averaged over an energy interval. As it is evident from Fig. 4, the two variables coincide reasonably well already at $b/a = 10$.

6. Conclusion

We considered a superlattice with a unit cell allowing for resonant states. In this system, the dipole matrix element of the transitions between the lowest subband and one of the excited subbands significantly increases when the final subband approaches the energy of the resonant state, peaking up in the resonant subband. However, transitions to all subbands except the resonant one have a zero matrix element at one of the subband edges. The intraband absorption strength will demonstrate similar behaviour. The shape of the absorption peak corresponding to the resonant subband is strongly affected by the 'intrusion' of the quasi-localised states into the superlattice spectrum.

Acknowledgements

A.V.D. and R.K. would like to thank Prof. W. Nolting for his interest in this work and valuable discussions. A.V.D. is grateful to DAAD for the support of his stay at Humboldt University Berlin. A.V.D. and V.V.M. acknowledge partial support of the Russian Foundation for Basic Research and of the Foundation 'Universities of Russia: Basic Research'.

References

[1] V.P. Kaidanov, Yu. I., Ravich, Uspekhi Fiz, Nauk 145 (1985) 51.
[2] R.W. Pohl, Einführung in die Optik, Springer, Berlin, 1948, Section 122.
[3] W. Heitler, The Quantum Theory of Radiation, Oxford University Press, Oxford, 1944, Section 15 (Chapter III).
[4] S.D. Beneslavskii, A.V. Dmitriev, N.S. Salimov, JETP 92 (1987) 305.
[5] A.V. Dmitriev, Solid State Commun. 74 (1990) 237.
[6] A.V. Dmitriev, R. Keiper, V.V. Makeev, Semiconductor Sci. Technol. 11 (1996) 1791.
[7] B.F. Levine, J. Appl. Phys. 74 (1993) R1.
[8] G. Bastard, Phys. Rev. B 24 (1981) 5693.
[9] G. Bastard, Phys. Rev. B 25 (1982) 7584.
[10] Hung-Sik Cho, P.L. Prucnal, Phys. Rev. B 36 (1987) 3237.
[11] S. Flügge, Practical Quantum Mechanics, I and II, Springer, Berlin, 1971.
[12] W. Kohn, Phys. Rev. 115 (1959) 809.
[13] N.W. Ashcroft, N.D. Mermin, Solid State Phys, New York Holt, Rinehart and Winston, New York, 1976 (Chapter 10).
[14] W. Heitler, The Quantum Theory of Radiation, Oxford University Press, Oxford, 1944, Section 10 (Chapter III).
[15] H.A. Bethe, Intermediate Quantum Mechanics, Benjamin, New York, Amsterdam 1964 (Chapter 12).